Controlled Formation of Ni–B Amorphous Alloy Nanoarray via Ultrasound-assisted Reductant-infiltration Strategy

Xueying Chen, Zhiying Lou, Songhai Xie, Minghua Qiao,* Shirun Yan, Yuanlong Zhu, Kangnian Fan, and Heyong He*

Department of Chemistry and Shanghai Key Laboratory of Molecular Catalysis and Innovative Materials, Fudan University, Shanghai 200433, P. R. China

(Received January 5, 2006; CL-060003; E-mail: mhqiao@fudan.edu.cn, heyonghe@fudan.edu.cn)

An effective and facile strategy, ultrasound-assisted reductant-infiltration, was realized in the preparation of hexagonally packed Ni–B amorphous alloy nanoarray, which exhibits superior catalytic properties to their nanoparticle counterpart in selective hydrogenation of acetophenone to 1-phenylethanol.

Recently, amorphous metal–metalloid alloys with short-range ordering and long-range disordering structure have gained much attention of metallurgists, physicists, and chemists owing to their special physical and chemical properties.[1,2] Some amorphous alloys, e.g., Ni–B, have superior catalytic properties such as higher activity, better selectivity, and stronger sulfur resistance in heterogeneous catalysis.[3–5] On the other hand, the systematic manipulation of the morphologies of nanoscale materials has always been a significant challenge in modern materials chemistry. When the shapes of nanoscale materials are transformed from usual spherical particles to one-dimensional (1D) nanowires or nanorods,[6] two-dimensional (2D) nanofilms,[7] or three-dimensional (3D) nanoarrays,[8] these nanostructures usually bear unique properties in mesoscopic physics, electronics, and nanodevice fabrication. Although shape control over crystalline materials has been a common practice, such work is lacking for amorphous metal–metalloid alloys, whereas the combination of the amorphous structure of the metal–metalloid alloys with proper morphological manipulation is expected to produce functional materials promising in magnetics, electronics, and catalysis.

Nanocasting using mesostructured silica as hard template is one of the most common strategies for fabricating crystalline nanostructures.[8] The present preparation methods for amorphous metal–metalloid alloys usually lead to discrete nanoparticles in the channels or aggregates on the surface.[5,6] By scrutinizing the reduction process, we believe that the insufficient reductant in the channels and the retarded outer-diffusion of hydrogen are two main causes adverse to the formation of the replicated mesostructures of the hard template.

In this paper, we demonstrate a novel ultrasound-assisted reductant-infiltration method for the preparation of hexagonally packed Ni–B nanoarray. The high concentration of the reductant and ultrasonication ensure the complete filling of the reductant in the mesopores. Moreover, the addition of complexing ligands to the metal ions lowers the forming rate of hydrogen on one hand; on the other hand, ultrasonication facilitates the dissipation of hydrogen, thus minimizing the extrusion of the Ni–B deposited in the channels by hydrogen.

In a typical synthesis, SBA-15[9] (0.5 g, 40–60 mesh) was first immersed into a aqueous KBH_4 solution (3.0 M, 17.2 mmol) for 5 min. The mixture was ultrasonicated for another 5 min. The excessive solution was decanted, and the borohydride-infiltrated SBA-15 was added into the aqueous nickel citrocomplex solution (0.5 M, 5.0 mmol). The reduction mixture was also ultrasonicated until no bubbles were released. Then, the siliceous template was dissolved by 2 M NaOH and the product was washed with distilled water, ultrasonicated to remove residual sodium silicate adhered to the surface of the materials, centrifuged and finally kept in methanol for characterization and activity test.

Figure 1 shows the small angle XRD patterns of SBA-15, Ni–B/SBA-15, and Ni–B nanoarray. Ni–B/SBA-15 exhibits almost the same diffraction pattern as that of SBA-15, demonstrating that the mesostructure of SBA-15 is well retained during the preparation. After complete removal of the silica template, the Ni–B nanoarray still displayed well-resolved XRD peaks, strongly supporting the ordered arrangement of the Ni–B nanowires. The wide angle XRD pattern of the silica-free Ni–B nanoarray (inset in Figure 1) gives a broad peak at $2\theta \approx 45^\circ$, characteristic of its amorphous nature.[10] The chemical composition of the nanoarray is $Ni_{68.8}B_{31.2}$ by ICP analysis.

Figure 2 displays the N_2 isotherms and pore size distribution curves for SBA-15 and Ni–B samples. All three samples exhibited a type IV isotherm with hysteresis above P/P_0 of 0.4, revealing the presence of mesopores. The pore volume of Ni–B/SBA-15 decreased by ca. 54% relative to that of SBA-15, inferring the incorporation of Ni–B into the SBA-15 channels, which can be seen more clearly from the pore size distribution curves (inset in Figure 2). As for silica-free Ni–B nanoarray, a BET surface area as large as 265.9 $m^2 \cdot g^{-1}$ and a pore volume of 0.712 $cm^3 \cdot g^{-1}$ were observed, which are much larger than the Ni–B nanoparticles with a BET surface area of 47.9 $m^2 \cdot g^{-1}$ and a pore volume of 0.147 $cm^3 \cdot g^{-1}$. The narrow pore size distribution around 3.8 nm further confirmed the ordered arrangement of the Ni–B nanowires.

TEM image of the Ni–B/SBA-15 sample (Figure 3a) revealed that the framework of SBA-15 is intact after the incorpo-

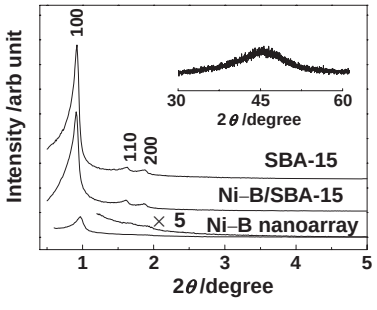

Figure 1. Small angle XRD patterns of SBA-15, Ni–B/SBA-15, and SBA-15-free 3D Ni–B nanoarray. Inset is wide angle XRD pattern of SBA-15-free 3D Ni–B nanoarray.

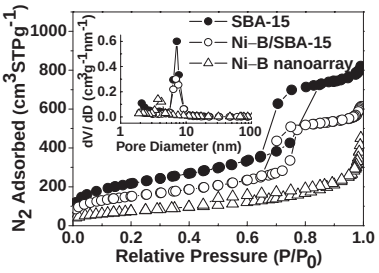

Figure 2. N_2 adsorption–desorption isotherms of SBA-15, Ni–B/SBA-15, and 3D Ni–B nanoarray. Inset shows the corresponding pore size distribution curves.

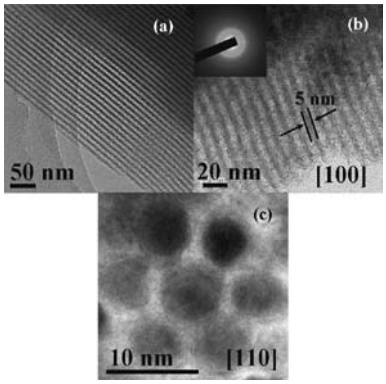

Figure 3. TEM images of (a) Ni–B/SBA-15 and (b and c) silica-free 3D Ni–B nanoarray. Inset in (b) shows the SAED pattern.

ration of Ni–B. Furthermore, the Ni–B nanowires are very uniform in diameter. As shown in Figures 3b and 3c, the silica-free Ni–B nanoarray is almost the replica of the mesostructure of SBA-15, and constructed by hexagonally packed nanowires with uniform diameter of ca. 5 nm. These nanowires are interconnected by even thinner Ni–B wires, originating from the micropores existed in SBA-15. EDX suggested that no silica was left in the Ni–B nanoarrays, verifying the complete removal of the template. The SAED pattern observed from the nanoarrays exhibited only diffraction halo (inset in Figure 3b), further confirming the amorphous nature of the Ni–B nanoarrays.[10]

The catalytic behavior of the as-prepared Ni–B nanoarray was explored using acetophenone (AP) hydrogenation as a probe. To the best of our knowledge, there has been no endeavor on the catalytic performance of the nanoarray materials. For comparison, Ni–B nanoparticles prepared under the same condition but without involving SBA-15 were tested. In a typical run, 10 mg of catalyst, 40 mL of methanol, and 0.1 mL of AP were added into a 75 mL teflon-lined stainless steel autoclave with a magnetic stirrer. The hydrogenation was carried out at 303 K with H_2 pressure of 3.0 MPa for 6 h. The products were analyzed by gas chromatography (GC122) with a CP-Chirasil-Dex CB capillary column and a FID detector.

Table 1 summarizes the conversion of AP, product selectivities, active surface areas, and turnover frequency (TOF) values of the two Ni–B materials. The 6 h-hydrogenation results show

Table 1. Hydrogenation of acetophenone over 3D Ni–B nanoarray (1) and Ni–B nanoparticle (2) materials

Catalyst	Conv. /mol %	Sel./mol %		S_H	TOF
		PE	CHMK	$/m^2\ g_{Ni}^{-1}$	/h
1	53.1	100	0	17.7	28.5
2	30.5	97.0	3.0	10.2	28.3

that 1-phenylethanol (PE, target product) was the only product over the Ni–B nanoarray, while over the Ni–B nanoparticle, 3.0% of AP was converted to cyclohexyl methyl ketone (CHMK), the aromatic ring hydrogenation product, suggesting that the Ni–B nanoarray is exclusively selective in saturating the carbonyl group. Moreover, the PE yield over the Ni–B nanoarray (53.1%) was much higher than that over the Ni–B nanoparticle (30.5 mol %), demonstrating the superior catalytic properties of the 3D Ni–B nanoarray material to Ni–B nanoparticles. It is an attractive behavior which requires further study.

In conclusion, a facile ultrasound-assisted reductant-infiltration strategy has been developed for the fabrication of amorphous Ni–B nanoarray with hexagonal mesostructures which is excellent catalyst in selective hydrogenation of acetophenone to 1-phenylethanol. We found that this strategy can be easily extended to other amorphous alloy nanostructures with various topologies.

This work was supported by the State Key Basic Research Development Program (No. G2000048009), the NSF of China (No. 20203004, 20025310, and 20421303), Shanghai Science and Technology Committee (No. 03QB14004), Cyrus Tang Innovation Fund and Graduate Innovation Foundation.

References

1 I. Bakonyi, A. Burgstaller, W. Socher, J. Voitlander, E. Tothkadar, A. Lovas, H. Ebert, E. Wachtel, N. Willmann, H. H. Liebermann, *Phys. Rev. B* **1993**, *47*, 14961.
2 T. Saito, M. Igarashi, M. Kobayashi, *J. Appl. Phys.* **2000**, *88*, 7209.
3 C. A. Brown, H. C. Brown, *J. Am. Chem. Soc.* **1963**, *85*, 1003.
4 Y. G. He, M. H. Qiao, H. R. Hu, J. F. Deng, K. N. Fan, *Appl. Catal., A* **2002**, *228*, 29.
5 X. Y. Chen, S. Wang, J. H. Zhuang, M. H. Qiao, K. N. Fan, H. Y. He, *J. Catal.* **2004**, *227*, 419.
6 Y. N. Xia, P. D. Yang, Y. G. Sun, Y. Y. Wu, B. Mayers, B. Gates, Y. D. Yin, F. Kim, Y. Q. Yan, *Adv. Mater.* **2003**, *15*, 353.
7 W. Weiss, W. Ranke, *Prog. Surf. Sci.* **2002**, *70*, 1.
8 a) F. Gao, Q. Y. Lu, D. Y. Zhao, *Adv. Mater.* **2003**, *15*, 739. b) K. K. Zhu, B. Yue, W. Z. Zhou, H. Y. He, *Chem. Commun.* **2003**, 98.
9 D. Y. Zhao, J. L. Feng, Q. S. Huo, N. Melosh, G. H. Fredrickson, B. F. Chmelka, G. D. Stucky, *Science* **1998**, *279*, 548.
10 J. van Wonterghem, S. Mørup, C. J. W. Koch, S. W. Charles, S. Wells, *Nature* **1986**, *322*, 622.

Published on the web (Advance View) March 11, 2006; DOI 10.1246/cl.2006.390